

# Hydrothermal Synthesis and Characterization of $[(\text{UO}_2)_2\text{F}_8(\text{H}_2\text{O})_2\text{Zn}_2(4,4'\text{-bpy})_2]\cdot(4,4'\text{-bpy})$ , a Mixed-Metal Uranyl Aquofluoride with a Pillared Layer Structure

Chih-Min Wang,<sup>†‡</sup> Chia-Hsien Liao,<sup>‡</sup> Hsien-Ming Kao,<sup>‡</sup> and Kwang-Hwa Lii<sup>\*†‡</sup>

*Institute of Chemistry, Academia Sinica, Nankang, Taipei, Taiwan 115, R.O.C., and Department of Chemistry, National Central University, Chungli, Taiwan 320, R.O.C.*

Received May 5, 2005

A mixed-metal uranyl aquofluoride,  $[(\text{UO}_2)_2\text{F}_8(\text{H}_2\text{O})_2\text{Zn}_2(4,4'\text{-bpy})_2]\cdot(4,4'\text{-bpy})$ , has been synthesized under hydrothermal conditions and has been structurally characterized by single-crystal X-ray diffraction, infrared spectroscopy, thermogravimetric analysis, emission spectroscopy, and solid-state NMR spectroscopy. It is one of the few uranium fluoride–organic framework solids in which an organic molecule is directly incorporated into the extended structure of the metal fluoride and is the first example of mixed-metal uranium oxyfluoride incorporating an organic ligand. The structure consists of neutral layers of edge- and corner-sharing uranium-centered pentagonal bipyramids and zinc-centered octahedra, which are linked through 4,4'-bpy ligands into a 3-D framework. The <sup>1</sup>H MAS NMR spectrum is in support of the conclusion that the occluded 4,4'-bpy molecules in the structural channels are not protonated. Crystal data: monoclinic, space group  $P2_1/c$ ,  $a = 9.4630(5)$  Å,  $b = 22.384(1)$  Å,  $c = 16.7534(8)$  Å,  $\beta = 91.899(2)^\circ$ ,  $V = 3546.7(4)$  Å<sup>3</sup> and  $Z = 4$ .

## Introduction

Uranium-bearing materials have been studied extensively because of their interesting coordination chemistry and diverse physical–chemical properties.<sup>1–3</sup> A large number of organically templated uranium fluorides and oxyfluorides with a wide variety of structures have recently been reported.<sup>4–16</sup> Most of them adopt either 1-D chain or 2-D

layer structures, while only a few have 3-D framework structures. Three mixed-metal uranium(IV) fluorides with 1-, 2-, and 3-D topologies which are created through the combination of U–F polyhedra with different isomers of  $\text{Ni}(\text{H}_2\text{O})_{6-x}\text{F}_x$  octahedra have also been reported.<sup>17</sup>

A good number of uranyl–organic framework solids have been synthesized by polymerizing U–O polyhedra through organic ligands. For example, the one-dimensional uranyl adipate,  $\text{UO}_2(\text{C}_6\text{H}_8\text{O}_4)(\text{H}_2\text{O})_2$ , consists of chains of  $(\text{UO}_2)\text{-O}_4(\text{H}_2\text{O})_2$  hexagonal bipyramids tethered through adipic acid. In contrast, the anhydrous phase,  $\text{UO}_2(\text{C}_6\text{H}_8\text{O}_4)$ , consists of edge-shared  $[(\text{UO}_2)_2\text{O}_8]$  dimers cross-linked by adipic acid into a neutral 3-D framework.<sup>18</sup> A series of uranyl dicarboxylates, in which mononuclear or dinuclear uranium

\* Author to whom correspondence should be addressed. E-mail: liikh@cc.ncu.edu.tw.

<sup>†</sup> Academia Sinica.

<sup>‡</sup> National Central University.

- (1) Doran, M. B.; Stuart, C. L.; Norquist, A. J.; O'Hare, D. *Chem. Mater.* **2004**, *16*, 565.
- (2) Kim, J.-Y.; Norquist, A. J.; O'Hare, D. *Chem. Mater.* **2003**, *15*, 1970.
- (3) Chen, W.; Yuan, H.-M.; Wang, J.-Y.; Liu, Z.-Y.; Xu, J.-J.; Yang, M.; Chen, J.-S. *J. Am. Chem. Soc.* **2003**, *125*, 9266.
- (4) Francis, R. J.; Halasyamani, P. S.; O'Hare, D. *Angew. Chem., Int. Ed.* **1998**, *37*, 2214.
- (5) Francis, R. J.; Halasyamani, P. S.; O'Hare, D. *Chem. Mater.* **1998**, *10*, 3131.
- (6) Francis, R. J.; Halasyamani, P. S.; Bee, J. S.; O'Hare, D. *J. Am. Chem. Soc.* **1999**, *121*, 1609.
- (7) Halasyamani, P. S.; Walker, S. M.; O'Hare, D. *J. Am. Chem. Soc.* **1999**, *121*, 7415.
- (8) Walker, S. M.; Halasyamani, P. S.; Allen, S.; O'Hare, D. *J. Am. Chem. Soc.* **1999**, *121*, 10513.
- (9) Allen, S.; Barlow, S.; Halasyamani, P. S.; Mosselmans, J. F. W.; O'Hare, D.; Walker, S. M.; Walton, R. I. *Inorg. Chem.* **2000**, *39*, 3791.
- (10) Talley, C. E.; Bean, A. C.; Albrecht-Schmitt, T. E. *Inorg. Chem.* **2000**, *39*, 5174.

- (11) Almond, P. M.; Deakin, L.; Porter, M. J.; Mar, A.; Albrecht-Schmitt, T. E. *Chem. Mater.* **2000**, *12*, 3208.
- (12) Almond, P. M.; Talley, C. E.; Bean, A. C.; Peper, S. M.; Albrecht-Schmitt, T. E. *J. Solid State Chem.* **2000**, *154*, 635.
- (13) Almond, P. M.; Deakin, L.; Mar, A.; Albrecht-Schmitt, T. E. *Inorg. Chem.* **2001**, *40*, 886.
- (14) Cahill, C. L.; Burns, P. C. *Inorg. Chem.* **2001**, *40*, 1347.
- (15) Almond, P. M.; Deakin, L.; Mar, A.; Albrecht-Schmitt, T. E. *J. Solid State Chem.* **2001**, *158*, 87.
- (16) Wang, C.-M.; Liao, C.-H.; Lin, H.-M.; Lii, K.-H. *Inorg. Chem.* **2004**, *43*, 8239.
- (17) Bean, A. C.; Sullens, T. A.; Runde, W.; Albrecht-Schmitt, T. E. *Inorg. Chem.* **2003**, *42*, 2628.
- (18) Borkowski, L. A.; Cahill, C. L. *Inorg. Chem.* **2003**, *42*, 7041.

building units are connected by bidentate anions such as succinate, glutarate, and isophthanlate, were reported.<sup>19</sup> The uranyl–nickel–organic hybrid compound,  $[\text{Ni}_2(\text{H}_2\text{O})_2(\text{QA})_2\text{-}(\text{bpy})_2\text{U}_5\text{O}_{14}(\text{H}_2\text{O})_2(\text{OAc})_2]\cdot 2\text{H}_2\text{O}$  ( $\text{H}_2\text{QA}$  = quinolinic acid), has a 3-D framework structure constructed from U–O ribbons and Ni–bpy layers linked through QA ligands.<sup>20</sup> Although a large number of organically templated uranium fluorides and oxyfluorides and uranyl–organic framework solids have been reported, few uranyl fluoride–organic framework solids in which organic molecules are directly incorporated into the extended structures of the metal fluorides are known. Recently, Kim et al. synthesized several uranyl fluoride isonicotinate with 1- and 2-D topologies in the uranyl acetates/HF/isonicotinic acid system.<sup>2</sup> The 1-D compounds consist of chains of edge-sharing uranium-centered pentagonal bipyramids with isonicotinate ligands separating the chains or with isonicotinic acid forming a hydrogen-bonded network. The 2-D compound consists of uranium oxyfluoride layers containing an eight-membered ring aperture with the isonicotinate ligands above and below the aperture. Following the successful synthesis of an organically templated mixed-valence uranium oxyfluoride with a hybrid network structure,<sup>16</sup> we report in this paper the first example of mixed-metal uranyl aquofluoride incorporating an organic ligand,  $[(\text{UO}_2)_2\text{F}_8(\text{H}_2\text{O})_2\text{Zn}_2(4,4'\text{-bpy})_2]\cdot (4,4'\text{-bpy})$  (bpy = bipyridine) (denoted as **1**). The synthesis, crystal structure, infrared spectroscopy, thermogravimetric analysis, emission spectroscopy, and solid-state NMR spectroscopy are reported.

## Experimental Section

**Synthesis and Initial Characterization.** Light-yellow block crystals of **1** were obtained in a yield of 81% on the basis of uranium acetate by heating a mixture of 0.25 mmol of  $\text{UO}_2(\text{CH}_3\text{COO})_2\cdot 2\text{H}_2\text{O}$  (Emsdiam, 99.6%), 0.5 mmol of  $\text{Zn}(\text{NO}_3)_2\cdot 6\text{H}_2\text{O}$  (Aldrich, 98%), 6 mmol of  $\text{HF}_{(\text{aq})}$  (Merck, 40% solution), 1.5 mmol of 4,4'-bpy (Acros, 98%), and  $\text{H}_2\text{O}$  (5.5 mL) in a Teflon-lined, 23-mL autoclave at 180 °C for 3 d followed by slow cooling at 6 °C  $\text{h}^{-1}$  to room temperature. The pH values of the solution before and after the hydrothermal reaction were 4 and 3, respectively, as indicated by pH paper. Powder X-ray data were collected on a Philips X'Pert Pro MPD X-ray diffractometer with  $\text{Cu K}\alpha$  radiation equipped with a X'Celerator detector. The X-ray powder pattern of the bulk product is in good agreement with the calculated pattern on the basis of the results from single-crystal X-ray diffraction (Figure S1). The CHN and fluorine elemental analysis (ion chromatography) results are consistent with the formula (anal. found/calcd: C, 27.23/27.14; H, 2.09/2.13; N, 6.35/6.33; F, 10.9/11.45).

The IR spectrum was recorded on a BIO-RAD FT-IR spectrometer within the range of 400–4000  $\text{cm}^{-1}$  using the KBr pellet method. Thermogravimetric analysis (TGA), using a Perkin-Elmer TGA7 thermal analyzer, was performed on a powder sample in flowing air in the temperature range of 40–900 °C with a heating rate of 5 °C  $\text{min}^{-1}$ . The emission of yellow-green light from **1** is easily observed when the sample is irradiated with 365-nm UV

light using a handheld UV lamp. Photoluminescence measurements were performed on a Hitachi F-4500 FL spectrophotometer with a 150 W Xe lamp as the excitation light source (360 nm) at room temperature using a 390-nm emission cutoff filter to suppress any scattered light from the source.

**Single-Crystal X-ray Diffraction.** A light-yellow crystal of dimensions  $0.28 \times 0.18 \times 0.16 \text{ mm}^3$  was selected for indexing and intensity data collection on a Siemens Smart CCD diffractometer equipped with a normal focus, 3 kW sealed tube X-ray source. The number of observed unique reflections ( $F_o > 4 \sigma(F_o)$ ) is 8418 ( $2\theta_{\text{max}} = 63.84^\circ$ ,  $R_{\text{int}} = 0.0264$ ). Empirical absorption corrections were performed by using SADABS program for Siemens area detector ( $T_{\text{min,max}} = 0.440, 0.952$ ).<sup>21</sup> On the basis of systematic absences and successful solution and refinement of the structure, the space group was determined to be  $P2_1/c$  (No. 14). The structure was solved by direct methods: The metal atoms were first located and the C, N, O, and F atoms were found from difference Fourier maps. The structure contains linear, symmetrical  $\text{UO}_2^{2+}$  ions. In the beginning, all other donors to U and Zn were assumed to be F atoms. Bond-valence calculation indicated that the three terminal atoms were undersaturated and that all other atoms had values close to 1.<sup>22,23</sup> The terminal atoms bonded to U(2) and Zn(2) had a valence sum of 0.39 and 0.26, respectively, and were assigned to water oxygen. The presence of water molecules in the structure is supported by IR spectroscopy which displays two stretching vibrations in the 3300–3500  $\text{cm}^{-1}$  range. The terminal atom bonded to U(1) had a value of 0.58, and the bond distance is too short for this ligand to be water. We earlier refined the structure with an oxygen atom at this terminal position. The atom exhibited nonpositive definite atom displacement factor and very small equivalent isotropic atom displacement factor ( $U_{\text{eq}}$ ). The substitution of F for O resulted in a normal appearance of displacement ellipsoid except that the value of  $U_{\text{eq}}$  was 1.5–2 times of those for other F atoms. The valence sum of this atom can be satisfied by forming hydrogen bonds with water molecules [ $\text{F}(8)\cdots\text{O}(5) = 2.63 \text{ \AA}$ ,  $\text{F}(8)\cdots\text{O}(6) = 2.74 \text{ \AA}$ ]. The assignment of this terminal atom as fluorine instead of oxygen is supported by elemental analysis result which is in favor of eight instead of seven fluorine atoms per formula unit. To balance the charge, the uncoordinated 4,4'-bpy has to be a neutral molecule. At this point, a  $^1\text{H}$  MAS NMR spectrum was taken. It did not reveal any proton bonded to the pyridine nitrogen atom (see below). The H atoms of the water molecules which coordinate to U(2) and Zn(2) were located from difference Fourier maps. The H atoms which are bonded to C atoms were positioned geometrically and were refined using a riding model. The final cycles of least-squares refinement including the atomic coordinates and anisotropic thermal parameters of all non-hydrogen atoms converged at  $R_1 = 0.0192$ ,  $wR_2 = 0.0336$ , and  $S = 0.841$ .  $\Delta\rho_{\text{max, min}} = 1.28, -1.18 \text{ e}\cdot\text{\AA}^{-3}$ . Neutral-atom scattering factors were used for all the atoms. Anomalous dispersion and secondary extinction corrections were applied. All calculations were carried out with the PC version of the SHELXTL program package.<sup>24</sup> The crystallographic data are given in Table 1, and selected bond lengths and bond angles are given in Table 2.

**Solid-State NMR Measurements.**  $^1\text{H}$  MAS (magic-angle spinning) NMR spectrum was acquired on a Varian Infinityplus-500

(21) Sheldrick, G. M. *SADABS, Program for Siemens Area Detector Absorption Corrections*; University of Göttingen: Göttingen, Germany, 1997.

(22) Brese, N. E.; O'Keeffe, M. *Acta Crystallogr.* **1991**, *B47*, 192.

(23) Burns, P. C.; Ewing, R. C.; Hawthorne, F. C. *Can. Mineral.* **1997**, *35*, 1551.

(24) Sheldrick, G. M. *SHELXTL Programs*, version 5.1; Bruker AXS GmbH: Karlsruhe, Germany, 1998.

(19) Kim, J.-Y.; Norquist, A. J.; O'Hare, D. *J. Chem. Soc., Dalton Trans.* **2003**, 2813.

(20) Yu, Z.-T.; Liao, Z.-L.; Jiang, Y.-S.; Li, G.-H.; Li, G.-D.; Chen, J.-S. *Chem. Commun.* **2004**, 1814.

**Table 1.** Crystallographic Data for  $[(\text{UO}_2)_2\text{F}_8(\text{H}_2\text{O})_2\text{Zn}_2(4,4'\text{-bpy})_2]\cdot(4,4'\text{-bpy})$ 

chemical formula	$\text{C}_{30}\text{F}_8\text{H}_{28}\text{N}_6\text{O}_6\text{U}_2\text{Zn}_2$
$a/\text{\AA}$	9.4630(5)
$b/\text{\AA}$	22.384(1)
$c/\text{\AA}$	16.7534(8)
$\beta/^\circ$	91.899(2)
$V/\text{\AA}^3$	3546.7(4)
$Z$	4
formula weight	1327.38
space group	$P2_1/c$ (No. 14)
$T, ^\circ\text{C}$	23
$\lambda(\text{Mo K}\alpha), \text{\AA}$	0.71073
$D_{\text{calc}}, \text{g}\cdot\text{cm}^{-3}$	2.486
$\mu(\text{Mo K}\alpha), \text{cm}^{-1}$	105.3
$R_1^a$	0.0192
$wR_2^b$	0.0336

<sup>a</sup>  $R_1 = \sum||F_o| - |F_c||/\sum|F_o|$ . <sup>b</sup>  $wR_2 = [\sum w(F_o^2 - F_c^2)^2/\sum w(F_o^2)]^{1/2}$ ,  $w = 1/[\sigma^2(F_o^2) + (aP)^2 + bP]$ ,  $P = [\max(F_o, 0) + 2(F_c)^2]/3$ , where  $a = 0.0113$  and  $b = 0$ .

**Table 2.** Selected Bond Lengths and Bond Angles for  $[(\text{UO}_2)_2\text{F}_8(\text{H}_2\text{O})_2\text{Zn}_2(4,4'\text{-bpy})_2]\cdot(4,4'\text{-bpy})$ 

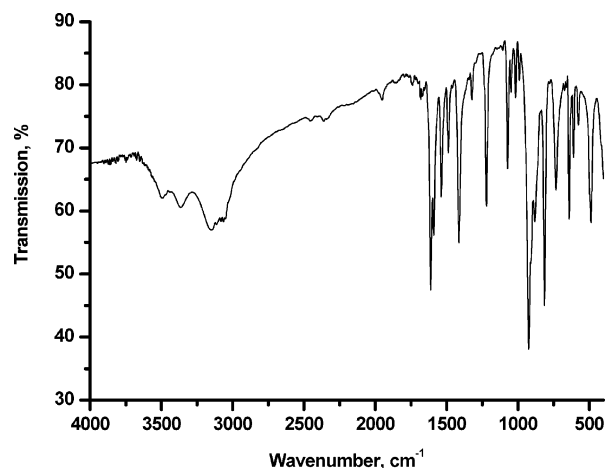
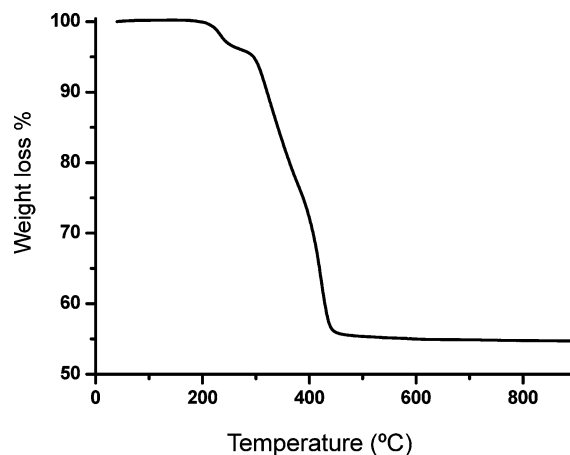
Bond Lengths (Å)			
U(1)–O(1)	1.773(2)	U(1)–O(2)	1.773(2)
U(1)–F(1)	2.303(1)	U(1)–F(2)	2.256(1)
U(1)–F(3)	2.291(1)	U(1)–F(4)	2.492(1)
U(1)–F(5)	2.244(1)	U(2)–O(3)	1.776(2)
U(2)–O(4)	1.771(2)	U(2)–O(5)	2.449(2)
U(2)–F(1)	2.325(1)	U(2)–F(4)	2.372(1)
U(2)–F(6)	2.259(1)	U(2)–F(7)	2.225(1)
Zn(1)–N(1)	2.076(2)	Zn(1)–N(3)	2.081(2)
Zn(1)–F(3)	2.112(1)	Zn(1)–F(4)	2.176(1)
Zn(1)–F(7)	1.974(2)	Zn(1)–F(8)	1.999(1)
Zn(2)–N(2)	2.107(2)	Zn(2)–N(4)	2.102(2)
Zn(2)–O(6)	2.103(2)	Zn(2)–F(2)	2.089(1)
Zn(2)–F(6)	2.090(1)	Zn(2)–F(8)	2.083(1)
O(5)–H(5A)	0.862	O(5)–H(5B)	0.775
O(6)–H(6A)	0.829	O(6)–H(6B)	0.752
Bond Angles (°)			
U(1)–F(1)–U(2)	119.52(6)	U(1)–F(2)–Zn(2)	156.56(6)
U(1)–F(3)–Zn(1)	110.64(5)	U(1)–F(4)–U(2)	110.59(5)
U(1)–F(4)–Zn(1)	101.60(5)	U(2)–F(4)–Zn(1)	147.79(6)
U(2)–F(6)–Zn(2)	156.67(7)	U(2)–F(7)–Zn(1)	154.97(7)
Zn(1)–F(8)–Zn(2)	136.74(7)		

NMR spectrometer equipped with a 2.5-mm Chemagnetics probe. A  $\pi/2$  pulse width of 4  $\mu\text{s}$ , a repetition time of 2 s, and a spinning speed of 28 kHz were used to acquire the  $^1\text{H}$  NMR spectra. A spin-echo pulse sequence with various evolution times ( $\tau$ ) was also used to eliminate the background signals from the probe head.  $^1\text{H}$  chemical shifts were externally referenced to tetramethylsilane (TMS) at 0 ppm.

## Results and Discussion

**Characterization.** In the IR spectrum of **1** (Figure 1), we find two O–H stretching absorptions at 3490 and 3350  $\text{cm}^{-1}$ . The ring C–H out-of-plane bending, ring C–C (or C–N) stretching, and ring C–H stretching absorptions are observed at 810, 1075, 1220, 1420, 1540, 1590, and  $\sim 3100$   $\text{cm}^{-1}$ . The sharp and intense band at 925  $\text{cm}^{-1}$  is due to asymmetric stretch of  $\text{UO}_2^{2+}$ . A medium band at 872  $\text{cm}^{-1}$  can be ascribed to symmetric  $\text{UO}_2^{2+}$  stretch because the uranyl units are not strictly linear. Therefore, the spectrum confirms the presence of  $\text{H}_2\text{O}$ , 4,4'-bpy, and uranyl group in **1**.

The TGA curve (Figure 2) shows weight loss in two overlapping steps, which begins at about 200  $^\circ\text{C}$  and is

**Figure 1.** Infrared spectrum of **1** (KBr pellet method).**Figure 2.** Thermogravimetric analysis of **1** in flowing air at 5  $^\circ\text{C min}^{-1}$ .

complete at about 450  $^\circ\text{C}$ . The first step (200 to  $\sim 250$   $^\circ\text{C}$ ) corresponds to the loss of two water molecules (obsd  $\sim 3.0\%$ , two  $\text{H}_2\text{O}$  calcd 2.71%). The observed total weight loss (45%) agrees well with the calculated value of 45.4% for the loss of two  $\text{H}_2\text{O}$ , four  $\text{F}_2$ , and three bpy molecules per formula unit. The X-ray powder pattern of the final decomposition product from TG analysis shows the presence of  $\text{ZnU}_3\text{O}_{10}$  (JCPDS-44-0915) and a small amount of unidentified product.

The emission spectrum for compound **1** shows the characteristic vibronic structure of the  $\text{UO}_2^{2+}$  moiety (Figure S2). The spectrum is consistent with those obtained for other uranyl-containing materials.<sup>12,25</sup> The five characteristic peaks range from about 505 to 605 nm, and the reason each peak has a shoulder is due to two crystallographically unique uranyl groups in the structure.

**Structure.** Two distinct uranium atoms are observed in the structure, each of which is seven-coordinate in pentagonal bipyramidal geometry (Figure 3). Each uranium(VI) cation is axially bonded to two oxide ligands through short “uranyl” bonds. The  $\text{UO}_2^{2+}$  units exhibit U–O bond lengths ranging between 1.772(2) and 1.778(2) Å and O–U–O bond angles of 177.86(9) and 178.40(9) $^\circ$ . Equatorially, U(1) is bonded

(25) Bean, A. C.; Peper, S. M.; Albrecht-Schmitt, T. E. *Chem. Mater.* **2001**, *13*, 1266.



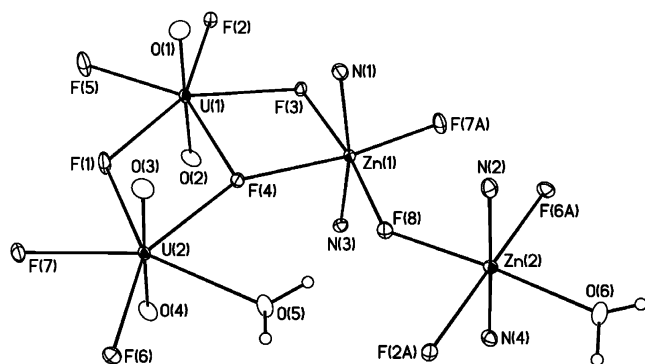


**Figure 3.** Coordination environments of metal atoms in **1** showing the atom labeling scheme. Small open circles are H atoms. Thermal ellipsoids are shown at 50% probability.

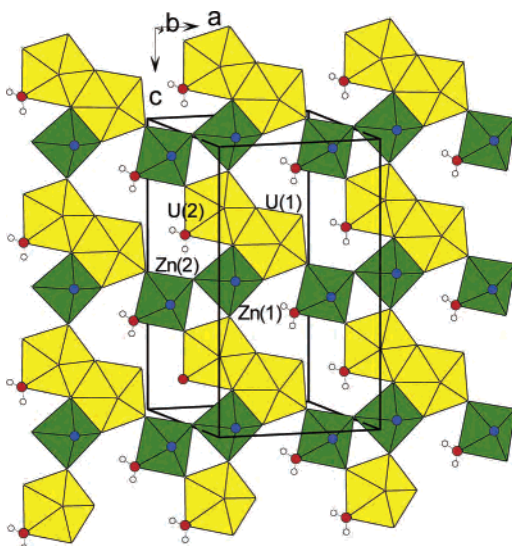


**Figure 4.** Section of an inorganic layer in **1**. Blue circles, N atoms; red circles, water oxygen atoms; small open circles, H atoms.

to five fluorine atoms, four of which bridge to adjacent U(2) and Zn atoms, with the U–F bond lengths ranging from 2.247(2) to 2.488(2) Å, whereas the fifth fluorine is terminal (U–F(2) = 2.247(2) Å). The equatorial coordination around U(2) contains one water molecule and four fluorine atoms with the U–F bond lengths ranging between 2.226(2) and 2.372(2) Å. The U–O distance for the coordinated water molecule is 2.458(2) Å, which is comparable to those (2.490(9) and 2.452(9) Å) in  $[\text{N}_2\text{C}_6\text{H}_{14}][(\text{UO}_2)_6(\text{H}_2\text{O})_2\text{F}_2(\text{PO}_4)_2(\text{HPO}_4)_4]\cdot 4\text{H}_2\text{O}$ .<sup>1</sup> The  $\text{UO}_2\text{F}_5$  pentagonal bipyramid is common, whereas the  $\text{UO}_2\text{F}_4(\text{H}_2\text{O})$  unit is observed for the first time. Both Zn atoms are six-coordinate in octahedral geometry with two pyridine nitrogen atoms in trans positions. Equatorially, Zn(1) is bonded to four fluorine atoms, whereas Zn(2) is bonded to three fluorine atoms and one water molecule. The Zn–O(aquo) distance (2.103(2) Å) is comparable to those in the literature.<sup>26,27</sup>

As shown in Figure 4, each dimer of edge-sharing uranium-centered pentagonal bipyramids shares an edge and three corners with three dimers of corner-sharing zinc-

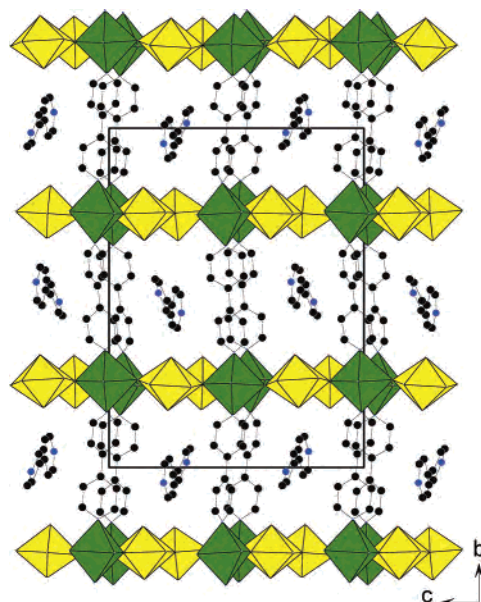


**Figure 5.** Structure of **1** viewed along the *a* axis. The yellow and green polyhedra are U-centered pentagonal bipyramids and Zn-centered octahedra, respectively. Black circles, C atoms; blue circles, N atoms. H atoms are not shown for clarity.

centered octahedra to form neutral layers in the *ac*-plane. The three bpy molecules in the asymmetric unit are present in two distinct forms: two as ligands to zinc and one in the free state. Adjacent layers are covalently linked through 4,4'-bpy ligands into a 3-D framework with rectangular channels that are occupied by neutral 4,4'-bpy molecules (Figure 5). All bpy molecules are not planar; the rings in bpy ligands are twisted at angles of 26.4° and 29.7°, and the angle for the uncoordinated bpy molecule is 25.4°. The occluded bpy molecule is oriented in a direction approximately orthogonal to neighboring bpy ligands. The dual role of 4,4'-bpy has been reported in the coordination polymer  $[\text{Cu}(4,4'\text{-bpy})_2(\text{H}_2\text{O})_2](\text{ClO}_4)_4\cdot(4,4'\text{-H}_2\text{bpy})$  and in the vanadium phosphate  $(4,4'\text{-H}_2\text{bpy})[\text{V}_2(\text{HPO}_4)_4(4,4'\text{-bpy})_2]$ .<sup>28,29</sup> However, the uncoordinated 4,4'-bpy molecules in these two compounds are diprotonated.

**<sup>1</sup>H MAS NMR.** Figure 6a shows the one-pulse <sup>1</sup>H MAS NMR spectrum of **1**, along with the assignments to specified protons as indicated in the inset of the figure. Three major resonances are observed at 9.2, 6.6, and 4.2 ppm. The huge bump underneath is due to the background signals from the probe head. The resonances at 9.2 and 6.6 ppm are indicated from a comparison with the <sup>1</sup>H solution NMR spectrum of 4,4'-bpy molecule to be assigned to the (*H<sub>a</sub>*, *H<sub>a</sub>'*) and *H<sub>b</sub>* protons in the aromatic ring, respectively. However, the spectral resolution is not high enough to distinguish resonances from closely similar *H<sub>a</sub>* and *H<sub>a</sub>'* protons. The resonance at 4.2 ppm is ascribed to the protons of the water molecules. The spectrum was deconvoluted using three peaks and a background signal as shown with dashed lines in Figure 6a. The intensity ratio of the three resonances at 9.2, 6.6, and 4.2 ppm is equal to 3.01:3.01:1, which is in good

(26) Lei, C.; Mao, J.-G.; Sun, Y.-Q.; Song, J.-L. *Inorg. Chem.* **2004**, *43*, 1964.

(27) Neeraj, S.; Rao, C. N. R.; Cheetham, A. K. *J. Mater. Chem.* **2004**, *14*, 814.

(28) Tong, M.-L.; Ye, B.-H.; Cai, J.-W.; Chen, X.-M.; Ng, S. W. *Inorg. Chem.* **1998**, *37*, 2645.

(29) Huang, C.-H.; Huang, L.-H.; Lii, K.-H. *Inorg. Chem.* **2001**, *40*, 2625.

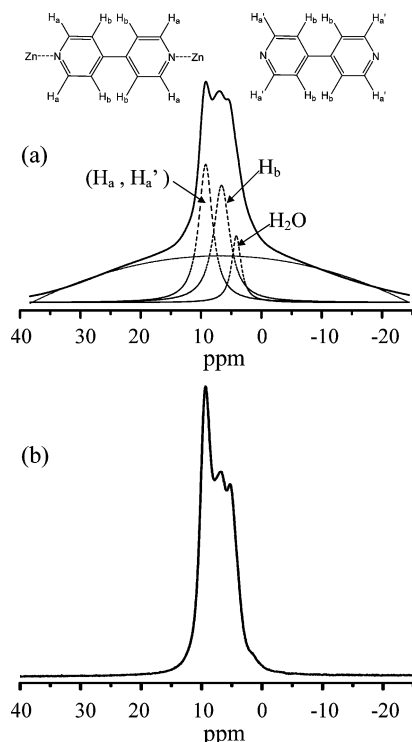


**Figure 6.** (a)  $^1\text{H}$  one-pulse MAS NMR spectrum of **1**, acquired at a spinning speed of 28 kHz and (b)  $^1\text{H}$  MAS NMR spectrum of **1**, acquired with a spin-echo pulse sequence with an evolution time of 10 rotor periods (i.e.,  $\tau = 357 \mu\text{s}$ ).

agreement with the stoichiometry of **1** (3:3:1) as determined from X-ray diffraction.

It would be expected that the proton bonded to pyridine nitrogen atom will be more deshielded compared with the proton bonded to carbon. For example, the  $^1\text{H}$  MAS NMR spectrum of  $[(\text{VO}_2)_2(4,4'\text{-bpy})_{0.5}(4,4'\text{-Hbpy})(\text{PO}_4)] \cdot \text{H}_2\text{O}$  exhibits four resonances at 14.2, 9.5, 7.2, and 3.7 ppm, corresponding to three different types of protons in 4,4'-bpy and 4,4'-Hbpy and one type of protons in  $\text{H}_2\text{O}$ . The peak at 14.2 ppm can be assigned to the proton bonded to the

pyridine nitrogen atom.<sup>30</sup> In the present case, the presence of this peak could be obscured by the background signals in the  $^1\text{H}$  one-pulse NMR spectrum. Therefore, a spin-echo pulse sequence with an evolution time of 10 rotor periods (i.e.,  $\tau = 357 \mu\text{s}$ ) was performed to eliminate the background signals. As shown in Figure 6b, the background signals were effectively removed, and the spectrum does not reveal any resonance near 14 ppm, which is in support of the conclusion that the occluded 4,4'-bpy molecules in the structural channels are not protonated.

In summary, we have synthesized a mixed-metal uranyl aquofluoride with a pillared layer structure. Although a large number of uranium fluorides and oxyfluorides have been reported, compound **1** is the first example of a mixed-metal uranium oxyfluoride incorporating an organic ligand. The 4,4'-bpy molecule is coordinated to two Zn atoms in adjacent layers to produce a 3-D framework. Bimetallic compounds are highly interesting because the second metal provides the possibility of incorporating organic ligands into the extended structures. Recently, we have synthesized another mixed-metal uranium fluoride with an unprecedented type of interpenetration by choosing an appropriate second metal and organic ligand.<sup>31</sup> Given the large variety of organic ligands and second metals that could be used in the synthesis, the scope for the synthesis of further mixed-metal uranium fluorides with novel structures appears to be very large.

**Acknowledgment.** We thank the National Science Council for support and Mr. Y.-S. Wen at the Institute of Chemistry, Academia Sinica for X-ray data collection.

**Supporting Information Available:** Crystallographic data for **1** in CIF format, X-ray powder patterns, and an emission spectrum. This material is available free of charge via the Internet at <http://pubs.acs.org>.

IC0507060

(30) Huang, L.-H.; Kao, H.-M.; Lii, K.-H. *Inorg. Chem.* **2002**, *41*, 2936.

(31) Wang, C.-M.; Lii, K.-H. Unpublished research at National Central University, 2005.